Available online at www.sciencedirect.com
SCIENCE DIRECT®
International Journal of Heat and Mass Transfer 47 (2004) 3415–3430
International Journal of HEAT and MASS TRANSFER
www.elsevier.com/locate/ijhmt

Analysis of heat and mass transfer in porous sorbents used in rotary regenerators

L.A. Sphaier, W.M. Worek *

Department of Mechanical and Industrial Engineering (M/C 251), University of Illinois at Chicago, 2039 Engineering Research Facility, 842 West Taylor Street, Chicago, IL 60607, USA

Received 25 April 2003; received in revised form 15 January 2004
Available online 24 March 2004

Abstract

A new dimensionless formulation, that locally accounts for heat conduction and mass diffusion in solid sorbent materials occurring in either enthalpy exchangers or desiccant wheels has been developed. Governing equations were fully normalized using classical dimensionless groups for heat and mass transfer. The model was validated using previously published results, including experimental data. The proposed equations are easily adaptable to incorporate additional features such as the influence of a supporting structure or the effects of flow entrance regions. Finally, results of a test-case are presented, indicating a possible optimization to wheel construction and compactness by reducing the felt thickness.

Keywords: Regenerator; Desiccant wheel; Enthalpy wheel; Dehumidification; Energy recovery

1. Introduction

The study of the transport phenomena occurring in rotary regenerators that employ sorbent materials has become an important aspect in designing these devices. Numerous investigations related to the mathematical modeling and method of solution associated with the problem of heat and mass transfer in regenerators have been conducted. Particularly interesting among the applications of regenerators are desiccant dehumidifiers, exhaustively investigated for over two decades [1–9], and enthalpy exchangers, which have been increasingly examined in the last years [10–13]. In addition, one should mention the studies [14–17], in which general formulations for heat and mass regenerators, regardless of the type of application, are presented. Also, a recent attempt to unify the formulations for desiccant and enthalpy wheels was presented by Niu and Zhang [18,19]. While most of these investigations comprise one-dimensional formulations with axial dependence only, using overall transfer coefficients to account for the transfer rates between the two phases, a few studies [6,7,9,18,19] employed two-dimensional formulations that actually consider the transport phenomena in felt; that is, as local diffusional processes.

Although considerable research has been individually devoted to either dehumidification or energy recovery applications, a complete unified formulation valid for both types of exchangers apparently is yet absent. The equations presented by Niu and Zhang [18,19] may indeed be employed for simulating both desiccant and enthalpy wheels; however, the normalization scheme adopted in those studies is rather limited, as dimensionless parameters—especially for the porous felt equations—presenting little physical significance were employed. In fact, this can be seen in various other investigations, some of which provide incomplete dimensionless analyses, normalizing only the independent variables. In addition, most of the studies related to desiccant or enthalpy wheels have been restricted to

* Corresponding author. Fax: +1-312-413-0447.
E-mail address: wworek@uic.edu (W.M. Worek).

0017-9310/$ - see front matter © 2004 Published by Elsevier Ltd.
doi:10.1016/j.ijheatmasstransfer.2004.01.016

Nomenclature

A	area
A_s	surface area
a	half of channel height
b	half of channel base width
c, c_p	specific heats
C	sensible heat capacity rate
$C^*_{r,f}$, C^*	sensible heat capacity ratios
CV	control volume
Bi	Biot number
$\mathscr{D}$	mass-diffusivity
D_p^H	hydraulic diameter
f_s	mass fraction of sorbent in felt
Fi_t, Fo_t	Fick and Fourier numbers
h	convective transfer coefficient
i	specific enthalpy
i_{vap}	latent heat of vaporization
i_w	differential heat of wetting
Δi_w	integral heat of wetting
i_{sor}	heat of sorption
$i_{v,\Delta T}$	interface heat of sorbate transfer
k	thermal conductivity
K_f	felt aspect ratio
L	channel length
Le	Lewis number
m, $\dot{m}$	mass and mass flow rate
n	number of channels in regenerator
N	number of revolutions
$N_{tu,o}$	overall number of transfer units
Nu	Nusselt number
P_p^n	wetted perimeter of one channel
r, x, t	independent variables
$2R_p$	channel spacing
ΔR_f	felt thickness
Sh	Sherwood number
T	temperature
u_p	bulk stream velocity in channels
u_{face}	velocity at inlet face
V	volumetric capacity rate
$V^*_{r,f}$, V^*	volumetric capacity ratios
W	sorbate uptake
Y	sorbate content in gas mixture

Greek symbols

ϵ_f	felt porosity
v_r	pore radius
Ω_{max}	dimensionless W_{fm}^{max}
Θ	dimensionless temperature
ρ	density or specific mass
ψ_r	psychrometric ratio
τ_t	period of one wheel revolution
τ_{dw}	dwell time
τ^*_{dw}	dimensionless dwell time
τ_g, τ_s	tortuosities
ϕ	molar fraction of sorbate in gas mixture
Φ	dimensionless sorbate concentration
φ_{sor}	dimensionless i_{sor}
$\varphi_{v,\Delta T}$	dimensionless $i_{v,\Delta T}$

Subscripts and superscripts

a	dry air
f	entire felt (matrix and pores)
fp	pores (inter-particle voids)
fm	matrix part of felt
p	process stream
fs	dry solid felt material
l	adsorbed liquid sorbate
ls	saturated liquid sorbate
v	saturated sorbate vapor
eff	effective property
ref	reference variable-value
*	dimensionless quantity
n	single channel structure
in, out	inlet and oulet
~	dry basis
–	average value
★	reference property-value
r	radial component
I, II	processes streams I and II
h	related to sensible heat transfer
m	related to mass transfer
i	related to enthalpy transfer
p.s.	process stream/felt interface
wall	supporting wall/felt interface

one-dimensional formulations [1,2,5,10,11,14,15,17], in which the unknown potentials depend on the axial coordinate and time only.

The purpose of the present investigation is to provide a complete and unified mathematical model for the transport process occurring in rotary-type exchangers, applicable for both energy exchange and dehumidification situations. This model includes gas-side and solid-side resistances to both heat and mass transfer as local diffusional processes, in which both gas-phase and surface diffusion are considered. Special attention is directed at the transfer processes within the porous felt and between the bulk process stream and the felt surface. A complete dimensionless formulation is also presented, involving physically meaningful characteristic parameters. Finally, the model is successfully validated against results from previous studies, including experimental data.

2. Mathematical modeling of transport problem

Fig. 1(a) illustrates a typical rotary regenerative exchanger. The rotary matrix revolves at a constant velocity ω, being cyclically exposed to two physically separated air streams, which can be either in counterflow or co-current arrangement. These streams, labeled *inlet-stream I* and *inlet-stream II*, are fed to the regenerator through two ducts, separated by a wedge to prevent mixing, thereby dividing the matrix into two flow-sections.

The rotary matrix is composed of numerous channels, parallel to the rotation axis, with relatively small cross-sectional areas. Because of the fixed sectioning, one can assume that at every instant a fixed fraction of the channels is subjected to inlet-stream I, while inlet-stream II is fed to the remaining fraction. Consequently, a flow-channel is said to be operating either in *period I* or *period II*, according to its current location. Regardless of the operating period, the fluid in channels will be simply referred to as *process stream* throughout this paper.

The transport phenomena occurring in these systems are usually analyzed by considering a single channel structure, bounded by an adiabatic and impermeable surface in the direction perpendicular to the process stream. This involves considering negligible radial and angular heat conduction between adjacent channels, which could be rather inappropriate, especially near the separating wedge, since the process stream in channels operating at different periods may present a considerable

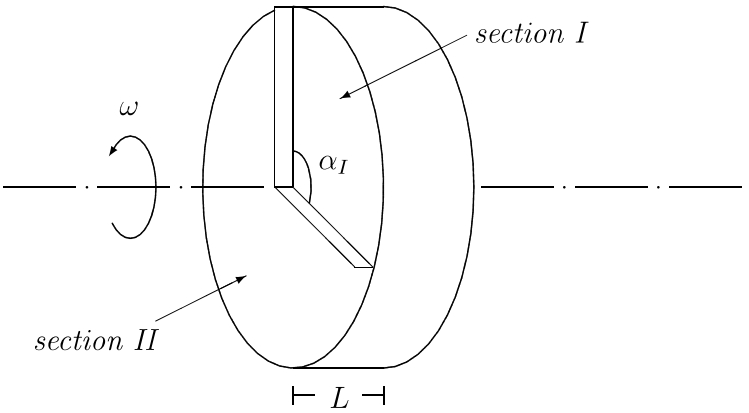

(a)

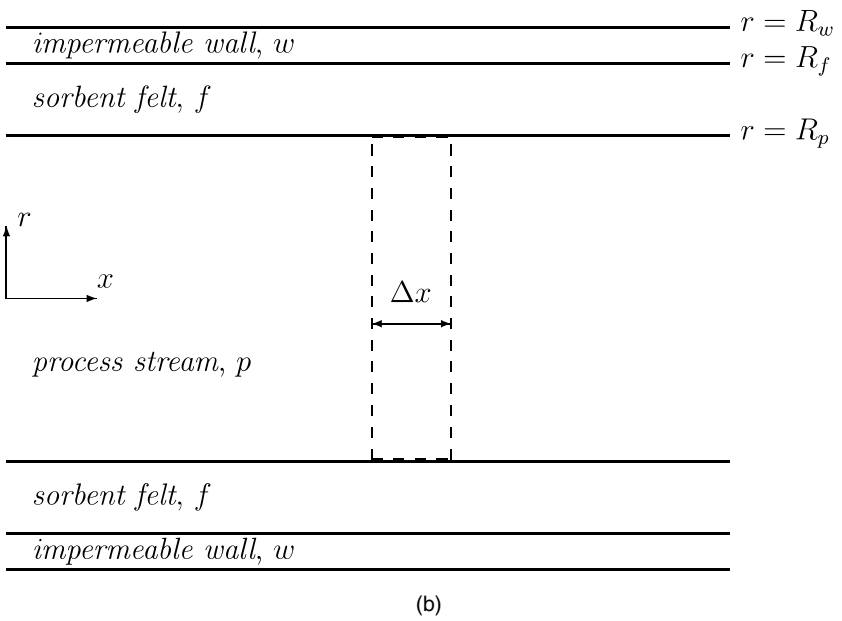

(b)

Fig. 1. System diagrams. (a) Rotary regenerator and (b) single flow-channel structure.

temperature difference. Nevertheless, this is a usual assumption among analyses of this type of problem; in addition, this issue becomes more relevant for slower rotational speeds, which are not the main focus of this investigation.

Despite the rotation, the channels are analyzed as stationary, by choosing a proper reference coordinate system, fixed to a representative channel. The walls of each channel are composed of a sorbent felt, or sorbent sheet, usually laid upon an impermeable supporting structure (Fig. 1(b)). Depending on the geometry of the channels, an exact representation of the system can be exceedingly complex, requiring a prohibitive computational effort for obtaining excessively detailed information. On the other hand, a description in terms of one dimensional models is overly simplified, since it cannot include accurate information about the diffusional effects that occur within the porous felt. A balance between these two extremes leads to a formulation that includes a reasonable amount of information, resulting in a feasible computational solution time, yet without compromising the accuracy of the description. In this formulation the cross-sectional diffusional effects in felt are considered in only one direction—normal to the felt surface. This involves considering negligible fluxes along the tangential direction, which is a reasonable assumption provided that curvature effects are small. Generally, one can expect that, if the wall and felt thickness are small compared to the hydraulic diameter, the transport rates can be accurately predicted by considering negligible curvature effects.

The porous felt is modeled as a homogeneous medium composed of a rigid matrix and pores, in which both gas and adsorbed liquid phases coexist. In order to facilitate the analysis, a subscripting scheme indicating the considered phase is employed. Starting with the rigid matrix, the subscript fm refers to quantities in this solid phase. Within pores, fp is employed. If for a given felt quantity no phase distinction is required, a simple f subscript is used. In the process stream and impermeable wall, a single-phase is present; thus, only one subscript is needed. These are p and w, respectively. In addition, sorbate concentrations are described employing mass ratios on dry-bases. For the gaseous phases, the variable Y is used, describing the mass of sorbate to that of the remaining components in the gas-mixture. For the liquid phase, the variable W describes the mass of liquid sorbate in the adsorbed phase, to that of dry sorbent. Furthermore, since the solid portion of the felt is composed of both sorbent and inert (i.e. non-adsorbent) materials, a quantity representing the mass fraction of sorbent in the felt is defined: f_s. Moreover, it is assumed that the inert fraction has no effects on sorption characteristics of the sorbent portion and no influence on the mechanism of surface diffusion, besides resulting in lower surface concentrations.

The idealizations that are implicit in the remaining sections of this study, are described below.

1. Radiation effects are neglected, as a result of relatively small temperatures.
2. No chemical reaction takes place, nor are there any energy sources within the system.
3. The effects of field forces, such as gravity, on the fluid mixture are negligible.
4. The channel flow is incompressible and viscous dissipation is negligible.
5. The channels are equal and uniformly distributed throughout the wheel.
6. The state properties of each inlet-stream are radially uniform at the inlet face of the wheel; also, the mass flow rate of dry air is constant at each inlet face.
7. Heat and mass transfer between adjacent flow-channels is negligible; heat and mass transfer from the exchanger to the surroundings (besides the channel inflow and outflow) are also negligible.
8. The pressure drop along the axial flow length due to skin friction is small compared to the total pressure, such that thermodynamic properties are unaffected.
9. All sorption phenomena are thermodynamically reversible.
10. Axial diffusion in the process stream is small compared to convective transfer, and is neglected.
11. The channel flow is laminar and fully developed; the convective heat and mass transfer between channels and the felt surface can be evaluated by employing bulk properties and film coefficients.
12. The gaseous components of the fluid mixture are treated as ideal gases with constant thermo-physical properties.
13. The concentration of fluid other than sorbate in the mixture is assumed constant.
14. The specific heats and thermal conductivities of dry sorbent and saturated liquid sorbate are assumed constant.
15. The gas mixtures are dilute solutions.
16. The porous felt is assumed to be homogeneous and isotropic, and the concentration of material other than sorbate is unaffected by sorption.
17. The mass diffusion rate in micro-pores is rapid compared to that of the macro-pores.
18. Thermodynamic equilibrium exists at every point between the sorbate in the gas-phase and in the solid.
19. No phase change, other than that related to the sorption process, occurs in the exchanger.
20. There is no explicit transfer coupling through *Soret* or *Dufor* effects [20].

Assumptions 5 and 6, together with 7, permit the channels to be independently treated, thereby significantly simplifying the analysis. Assumption 5 also pro-

vides a uniformly distributed transfer area throughout the wheel and, together with 6, ensures a constant and equal mass flow rate of dry air for all channels. The eighth assumption allows the energy balances to be written as enthalpy conservation equations once assumption 3 is also considered. Also, with assumption 9, one can express the sorbate uptake and all enthalpies as functions of temperatures and sorbate concentration in gas-phases. Assumption 10 is generally valid, because the heat and mass transfer Peclet numbers for gases are reasonably over 50. Furthermore, assumption 11 neglects the effect of a thermal entrance region, which for the current problem would be around 1/10 of the flow-channel length [11].

The level of uncertainty introduced by assumptions 12–14 will depend on the operation temperature range, since some properties present considerable dependence on temperature. This could be a problem especially in dehumidification, in which the elevated regeneration temperatures involved can generate variations of over 20% in some properties. In order to address this problem, besides using temperature-dependent expressions for some properties, an additional conservation equation (for the solvent) would be required, as considered in [11]. Nevertheless, as this work is focused on investigating the transport phenomena *within* the porous felt, an analysis including the temperature-dependence in these properties is out of the scope of this study. Once assumptions 13 and 15 are considered the analysis is simplified, since the solvent behaves as a transporting medium and the cross-sectional-averaged channel velocity can be regarded as constant.

Assumption 16 prevents the solid portion of the felt to swell upon adsorbing fluid or changing temperature, and in assumption 17, only the diffusion through the macro-pores of the solid felt is considered. In other words, this analysis is directed to cases in which macro-pore diffusion is controlling, and only sorbents possessing such characteristic are considered. Furthermore, in assumption 18, the kinetics of surface adsorption is considered fast enough to ensure local equilibrium within the felt. Finally, the 19th requires that the partial pressure of the gaseous sorbate remain below saturation, and assumption 20 guarantees that the mass transfer rates are not directly affected by thermal effects and vice-versa.

2.1. Thermo-physical properties, enthalpies, and heats of sorption

The densities of the fluid mixture in the process stream and pores and the density of the wet sorbent matrix are given by:

$$\rho_{\mathrm{p}} = \rho_{\mathrm{a}}(1 + Y_{\mathrm{p}}), \quad \rho_{\mathrm{fp}} = \rho_{\mathrm{a}}(1 + Y_{\mathrm{fp}}),$$
$$\rho_{\mathrm{fm}} = \rho_{\mathrm{fs}}(1 + f_{\mathrm{s}} W_{\mathrm{fm}}), \tag{1}$$

and the apparent density of the entire porous felt is given by:

$$\rho_{\mathrm{f}} = \epsilon_{\mathrm{f}} \rho_{\mathrm{fp}} + (1 - \epsilon_{\mathrm{f}}) \rho_{\mathrm{fm}}. \tag{2}$$

The specific heats for the process stream and sorbent felt are related through the following expressions:

$$\rho_{\mathrm{p}} c_{p_{\mathrm{p}}} = \rho_{\mathrm{a}} \tilde{c}_{p_{\mathrm{p}}}, \quad \rho_{\mathrm{f}} c_{\mathrm{f}} = \epsilon_{\mathrm{f}} \rho_{\mathrm{a}} \tilde{c}_{p_{\mathrm{fp}}} + (1 - \epsilon_{\mathrm{f}}) \rho_{\mathrm{fs}} \tilde{c}_{\mathrm{fm}}. \tag{3}$$

Assuming a simple parallel thermal resistance arrangement, the effective thermal conductivity of the felt is given by [21]:

$$k_{\mathrm{f,eff}} = \epsilon_{\mathrm{f}} k_{\mathrm{fp}} + (1 - \epsilon_{\mathrm{f}}) k_{\mathrm{fm}}. \tag{4}$$

The adsorption of vapor by the porous solid is conceptualized as a process consisting of the normal condensation followed by the formation of a thin liquid film over the solid surface. This liquid can be highly compressed, thereby causing its specific enthalpy to be at a lower level than that of *saturated-liquid* at the same temperature. This finite difference in enthalpy is denoted the *integral heat of wetting*. This concept also exists in differential form—denoted the *differential heat of wetting*, which is defined as the amount of energy released (per unit mass) as an infinitesimal amount of sorbate undergoes a change of state from saturated-liquid to adsorbed liquid. The differential and integral heats of wetting are easily related through:

$$\Delta i_{\mathrm{w}}(W, T) = \int_0^W i_{\mathrm{w}}(\omega, T)\, \mathrm{d}\omega, \tag{5}$$

and the integral heat of wetting is expressed as [22]:

$$\Delta i_{\mathrm{w}}(W, T) = i_{\mathrm{vap}}(T) \int_0^W \left(1 - \frac{i_{\mathrm{sor}}(w, T)}{i_{\mathrm{vap}}(T)}\right) \mathrm{d}w = \int_0^W \big(i_{\mathrm{vap}}(T) - i_{\mathrm{sor}}(w, T)\big) \mathrm{d}w, \tag{6}$$

where i_{sor} is the differential heat of sorption. Hence, one writes:

$$i_{\mathrm{w}} = \left(\frac{\partial \Delta i_{\mathrm{w}}}{\partial W}\right)_T = i_{\mathrm{vap}} - i_{\mathrm{sor}}. \tag{7}$$

As ideal gases are considered, it is necessary that the enthalpy of sorbate vapor equal that of saturated vapor at the same temperature. As a result, the heat of sorption is expressed as:

$$i_{\mathrm{sor}}(W, T) = i_{\mathrm{v}}(T) - i_{\mathrm{ls}}(T) - i_{\mathrm{w}}(W, T) = i_{\mathrm{v}}(T) - i_{\mathrm{l}}(W, T). \tag{8}$$

For the particular transport processes in the regenerator, the enthalpy of each phase is a function of sorbate concentration and temperature. For the three phases that constitute the physical domain, the enthalpies are given by:

$$\rho_a \tilde{i}_p = \rho_a (i_{a,p} + Y_p i_{v,p}), \quad \rho_a \tilde{i}_{fp} = \rho_a (i_{a,d} + Y_{fp} i_{v,d}), \tag{9}$$

$$\rho_{fs} \tilde{i}_{fm} = \rho_{fs} (i_{fs} + f_s (W_{fm} i_{ls} + \Delta i_w)). \tag{10}$$

According to the previous formulas, dry-basis specific heats are given by:

$$\tilde{c}_{p_p} = \frac{\partial \tilde{i}_p}{\partial T_p}, \quad \tilde{c}_{p_{fp}} = \frac{\partial \tilde{i}_{fp}}{\partial T_f}, \quad \tilde{c}_{fm} = \left(\frac{\partial \tilde{i}_{fm}}{\partial T_f} \right)_{W_{fm}}. \tag{11}$$

2.2. Governing equations for transport phenomena

2.2.1. Transport phenomena in process stream

Using a fixed control volume (Fig. 1), a sorbate mass-balance for the process stream yields:

$$\begin{aligned} &\{\text{rate of sorbate increase in CV}\}_1 \\ &\quad = \{\text{net sorbate influx by fluid flow}\}_2 \\ &\qquad - \{\text{sorbate transfer rate to felt}\}_3, \end{aligned} \tag{12}$$

where the involved terms are given by:

$$\{\ \}_1 = \frac{\partial}{\partial t} (A_p^n \Delta x \rho_a Y_p),$$

$$\{\ \}_2 = -\frac{\partial}{\partial x} (u_p A_p^n \rho_a Y_p) \Delta x, \tag{13}$$

$$\{\ \}_3 = (P^n \Delta x j''_{r,p})|_{p.s.} = P_p^n \Delta x (j''_{r,p})|_{p.s.}. \tag{14}$$

The energy balance is slightly more involved than the mass balance:

$$\begin{aligned} &\{\text{rate of enthalpy increase in CV}\}_1 \\ &\quad = \{\text{net enthalpy transfer (to CV)by fluid flow}\}_2 \\ &\qquad - \{\text{conduction heat transfer to felt}\}_3 \\ &\qquad - \{\text{energy decrease by sorbate transfer to felt}\}_4, \end{aligned} \tag{15}$$

where the indicated terms are written as:

$$\{\ \}_1 = \frac{\partial}{\partial t} (A_p^n \Delta x \rho_a \tilde{i}_p), \quad \{\ \}_2 = -\frac{\partial}{\partial x} (u_p A_p^n \rho_a \tilde{i}_p) \Delta x, \tag{16}$$

$$\{\ \}_3 = (P^n \Delta x q''_{r,p})|_{p.s.} = P_p^n \Delta x (q''_{r,p})|_{p.s.}, \tag{17}$$

$$\{\ \}_4 = (P^n \Delta x j''_{r,p} i_v)|_{p.s.} = P_p^n \Delta x (j''_{r,p})|_{p.s.} i_{v,p}. \tag{18}$$

As the molecular and thermal transport rates from the process stream to the felt are controlled by film resistances and since dilute gas-mixtures are considered [23], the heat and mass fluxes at this interface is given by:

$$\begin{aligned} (q''_{r,p})|_{p.s.} &= h_h (T_p - T_f|_{p.s.}), \\ (j''_{r,p})|_{p.s.} &= h_m \rho_a (Y_p - Y_{fp}|_{p.s.}). \end{aligned} \tag{19}$$

Substituting the equations for each term in the mass and energy balances into Eqs. (12) and (15), using Eq. (19), gives, after simplification:

$$\frac{DY_p}{Dt} = -\frac{4h_m}{D_p^H} (Y_p - Y_{fp}|_{p.s.}), \tag{20}$$

$$\rho_a \tilde{c}_{p_p} \frac{DT_p}{Dt} = -\frac{4h_h}{D_p^H} (T_p - T_f|_{p.s.}), \tag{21}$$

where D_p^H is the hydraulic diameter ($D_p^H = 4A_p^n/P_p^n = 4A_p/P_p$) and D/Dt denotes a material derivative, for this study expressed as:

$$\frac{D}{Dt} = \frac{\partial}{\partial t} + u_p \frac{\partial}{\partial x}. \tag{22}$$

2.2.2. Transport phenomena in sorbent felt

For the felt, an arbitrary, coordinate system independent, stationary control volume ΔV with bounding surface δS is considered, and a general mass conservation balance is written:

$$\begin{aligned} &\{\text{rate of sorbate increase in CV}\}_1 \\ &\quad = \{\text{net sorbate transfer into CV}\}_2 \end{aligned} \tag{23}$$

The storage term is written as the sum of the rates of increase of sorbate concentration in the gas-phase and in the adsorbed-phase:

$$\{\ \}_1 = \frac{\partial}{\partial t} \int_{\Delta V} \epsilon_f \rho_a Y_{fp} \, dv + \frac{\partial}{\partial t} \int_{\Delta V} (1 - \epsilon_f) \rho_{fs} f_s W_{fm} \, dv. \tag{24}$$

The net sorbate transfer is given by the net contributions of the independently parallel processes of gas-phase and surface diffusion:

$$\{\ \}_2 = -\int_{\delta S} \mathbf{j}''_{fp} \cdot \mathbf{n} \, ds - \int_{\delta S} \mathbf{j}''_{fm} \cdot \mathbf{n} \, ds. \tag{25}$$

Energy can be transported through the sorbent felt by means of heat conduction and sorbate transfer. Thus, a general energy balance in the CV is written in the following form:

$$\begin{aligned} &\{\text{rate of enthalpy increase in CV}\}_1 \\ &\quad = \{\text{net heat conduction into CV}\}_2 \\ &\qquad + \{\text{net heat flow into CV by mass transfer}\}_3. \end{aligned} \tag{26}$$

The enthalpy storage term is given by the sum of the rates of increase of enthalpy in the pores and matrix:

$$\{\ \}_1 = \frac{\partial}{\partial t} \int_{\Delta V} \epsilon_f \rho_a \tilde{i}_{fp} \, dv + \frac{\partial}{\partial t} \int_{\Delta V} (1 - \epsilon_f) \rho_{fs} \tilde{i}_{fm} \, dv. \tag{27}$$

The net heat entering the control volume by conduction and mass transfer is given by adding the contributions of each energy influx integrated around the volume element:

$$\{\ \}_2 = -\int_{\delta S} \mathbf{q}''_{\mathrm{f}} \cdot \mathbf{n}\,\mathrm{d}s,$$

$$\{\ \}_3 = -\int_{\delta S} \mathbf{j}''_{\mathrm{fp}} \cdot \mathbf{n} i_{\mathrm{v,d}}\,\mathrm{d}s - \int_{\delta S} \mathbf{j}''_{\mathrm{fm}} \cdot \mathbf{n} i_{\mathrm{l}}\,\mathrm{d}s. \tag{28}$$

In order to obtain the heat and concentration fluxes within the sorbent felt, Fourier's law, Fick's law for binary solutions, and a Fick's-law type expression [24] are employed:

$$\mathbf{j}''_{\mathrm{fp}} = -\frac{\mathscr{D}_{\mathrm{g}}\epsilon_{\mathrm{f}}}{\tau_{\mathrm{g}}}\nabla(\rho_{\mathrm{a}} Y_{\mathrm{fp}}), \quad \mathbf{j}''_{\mathrm{fm}} = -\frac{\mathscr{D}_{\mathrm{s}}}{\tau_{\mathrm{s}}}\nabla(\rho_{\mathrm{fs}}(1-\epsilon_{\mathrm{f}}) f_{\mathrm{s}} W_{\mathrm{fm}}),$$
$$\mathbf{q}''_{\mathrm{f}} = -k_{\mathrm{f,eff}}\nabla T_{\mathrm{f}}. \tag{29}$$

Substituting the equations for each term in the mass and energy balances into Eqs. (23) and (26), using Eq. (29), and eliminating negligible terms, gives, after simplification:

$$\epsilon_{\mathrm{f}}\rho_{\mathrm{a}}\frac{\partial Y_{\mathrm{fp}}}{\partial t} + (1-\epsilon_{\mathrm{f}})\rho_{\mathrm{fs}} f_{\mathrm{s}}\frac{\partial W_{\mathrm{fm}}}{\partial t} = \rho_{\mathrm{a}}\nabla\cdot(\mathscr{D}_{\mathrm{g,eff}}\nabla Y_{\mathrm{fp}}) + \rho_{\mathrm{fs}} f_{\mathrm{s}}\nabla\cdot(\mathscr{D}_{\mathrm{s,eff}}\nabla W_{\mathrm{fm}}), \tag{30}$$

$$\rho_{\mathrm{f}} c_{\mathrm{f}}\frac{\partial T_{\mathrm{f}}}{\partial t} = \nabla\cdot(k_{\mathrm{f,eff}}\nabla T_{\mathrm{f}}) + \rho_{\mathrm{fs}} f_{\mathrm{s}}\left((1-\epsilon_{\mathrm{f}})\frac{\partial W_{\mathrm{fm}}}{\partial t} - \nabla\cdot(\mathscr{D}_{\mathrm{s,eff}}\nabla W_{\mathrm{fm}})\right) i_{\mathrm{sor}}, \tag{31}$$

where the effective diffusivities are defined as:

$$\mathscr{D}_{\mathrm{g,eff}} = \frac{\epsilon_{\mathrm{f}}\mathscr{D}_{\mathrm{g}}}{\tau_{\mathrm{g}}}, \quad \mathscr{D}_{\mathrm{s,eff}} = \frac{(1-\epsilon_{\mathrm{f}})\mathscr{D}_{\mathrm{s}}}{\tau_{\mathrm{s}}}. \tag{32}$$

2.2.3. Boundary conditions and equilibrium relation

Boundary conditions are obtained thought interface balances, resulting in the following equations:

$$-\rho_{\mathrm{a}}\mathscr{D}_{\mathrm{g,eff}}\frac{\partial Y_{\mathrm{fp}}}{\partial r} - \rho_{\mathrm{fs}}\mathscr{D}_{\mathrm{s,eff}}\frac{\partial W_{\mathrm{fm}}}{\partial r} = h_{\mathrm{m}}\rho_{\mathrm{a}}(Y_{\mathrm{p}} - Y_{\mathrm{fp}}), \quad \text{at} \quad r = R_{\mathrm{p}}, \tag{33}$$

$$-k_{\mathrm{f,eff}}\frac{\partial T_{\mathrm{f}}}{\partial r} = h_{\mathrm{h}}(T_{\mathrm{p}} - T_{\mathrm{f}}) + h_{\mathrm{m}}\rho_{\mathrm{a}}(Y_{\mathrm{p}} - Y_{\mathrm{fp}}) i_{\mathrm{v},\Delta T} - \rho_{\mathrm{fs}}\mathscr{D}_{\mathrm{s,eff}} f_{\mathrm{s}}\frac{\partial W_{\mathrm{fm}}}{\partial r} i_{\mathrm{sor}}, \quad \text{at} \quad r = R_{\mathrm{p}}, \tag{34}$$

$$\left(-\rho_{\mathrm{a}}\mathscr{D}_{\mathrm{g,eff}}\frac{\partial Y_{\mathrm{fp}}}{\partial r} - \rho_{\mathrm{fs}}\mathscr{D}_{\mathrm{s,eff}} f_{\mathrm{s}}\frac{\partial W_{\mathrm{fm}}}{\partial r}\right)\Bigg|_{\mathrm{wall}} = 0, \tag{35}$$

$$\left(-k_{\mathrm{f,eff}}\frac{\partial T_{\mathrm{f}}}{\partial r} - \rho_{\mathrm{a}}\mathscr{D}_{\mathrm{g,eff}}\frac{\partial Y_{\mathrm{fp}}}{\partial r} i_{\mathrm{v,d}} - \rho_{\mathrm{fs}}\mathscr{D}_{\mathrm{s,eff}} f_{\mathrm{s}}\frac{\partial W_{\mathrm{fm}}}{\partial r} i_{\mathrm{l}}\right)\Bigg|_{\mathrm{wall}} = (q''_{\mathrm{w,r}})|_{\mathrm{wall}}, \tag{36}$$

where $i_{\mathrm{v},\Delta T}$ is termed the *heat of sorbate transfer at the interface*, which is given by:

$$i_{\mathrm{v},\Delta T} = c_{p_{\mathrm{v}}}(T_{\mathrm{p}} - T_d). \tag{37}$$

At $x = 0$ and $x = L$, the transfer areas correspond to less than 0.1% of the total [11]; thus, one may assume insulated and impermeable boundaries at these ends with negligible errors, leading to:

$$\frac{\partial T_{\mathrm{f}}}{\partial x} = \frac{\partial Y_{\mathrm{fp}}}{\partial x} = 0, \quad \text{at} \quad x = 0, L. \tag{38}$$

The last set of boundary conditions involve the inlet conditions for the process stream, which are given by periodic Dirichlet boundary conditions, and are provided together with the dimensionless formulation. In addition, since for these applications quasi-steady-state solutions are sought, initial conditions are not critical, and will be ignored for the time being.

The initial-boundary-value problem derived in the foregoing sections is completed, by selecting an *equilibrium relation*, or *equilibrium isotherm*. This relation is locally applied within the felt, and written in the following general form:

$$W_{\mathrm{fm}} = W_{\mathrm{fm}}(T_{\mathrm{f}}, Y_{\mathrm{fp}}), \quad \text{with} \quad 0 \leqslant W_{\mathrm{fm}}(T_{\mathrm{f}}, Y_{\mathrm{fp}}) \leqslant W_{\mathrm{fm}}^{\max}. \tag{39}$$

The proposed governing equations together with the boundary conditions and the equilibrium relation, constitute a system of PDEs that can be applied for the simulation of several configurations. Since the diffusional terms in felt equations (30) and (31) are given in vector form, both heat conduction and mass diffusion in all spatial variables are considered. In fact, these equations can be readily used as three dimensional ones, as well as with different coordinate systems, provided that the boundary conditions are modified. Although this work focuses on the two-dimensional form of the equations, the vector notation is preserved because of its simplicity.

Despite the fact that some investigations include the effects of the impermeable supporting structure, this analysis is narrowed to cases in which it is absent. This simplification is considered in order to permit a careful investigation of the transport phenomena within the porous felt, while avoiding an exceedingly lengthy discussion for the current space limitations. This simplification corresponds to considering an insulated boundary at $r = R_{\mathrm{f}}$, and it is easily shown that under this arrangement, the boundary conditions at the wall reduce to:

$$\left.\frac{\partial T_{\mathrm{f}}}{\partial r}\right|_{\mathrm{wall}} = \left.\frac{\partial Y_{\mathrm{fp}}}{\partial r}\right|_{\mathrm{wall}} = 0. \tag{40}$$

Regardless of this simplification, the analysis should provide reasonable insight into the transfer processes occurring within the porous felt. In addition, in order to incorporate the contribution of the supporting wall into the solution, one need only modify the boundary

conditions at the felt/wall interface and possibly consider additional equations, those of which would be similar to ones found in classical heat conduction texts [25].

Furthermore, it should be mentioned that, the boundary conditions for mass transfer at the impermeable surface must be written in the form of Eq. (35), in which the sum of the surface and gas-phase contributions results in a zero flux. Separately equating these fluxes at the supporting structure to zero—as it happens if there is no such structure—forces the energy condition at the same interface to yield $(q''_{w,r})|_{wall} = 0$, which cannot be true if a supporting wall is indeed considered.

3. Dimensionless formulation

While for isothermal mass transfer or sensible heat transfer dimensionless groups are well established and can be readily obtained, for regenerative coupled heat and mass transfer with adsorption only a limited amount of studies discuss the subject, most of which are focused on enthalpy exchangers. Especially interesting, is the work of Simonson and Besant [13], which provides a detailed description of dimensionless groups in a one-dimensional formulation involving enthalpy wheels.

In this paper, regenerative exchanger dimensionless groups for are defined following Shah [26], and some of the parameters obtained are similar those in [13]. Nevertheless, additional parameters relevant to heat and mass diffusion must be introduced due to the presence of these phenomena in the felt. In order to avoid dealing with variable dimensionless groups, all parameters are defined in terms of reference properties, and since the mass fractions of sorbate in the system are relatively small, "dry-properties" are used as reference values; that is, properties for a state of zero sorbate concentration. In addition, for temperature-dependent properties, temperature-averaged values are employed.

3.1. Reference values

The reference mass flow rates and the reference total mass of felt in the wheel are defined as:

$$(\dot{m}^{\star}_{p})|_{I} = \frac{\tau_{I}}{\tau_{t}}\rho^{\star}_{p}u_{p,I}A_{p},$$
$$(\dot{m}^{\star}_{p})|_{II} = \frac{\tau_{II}}{\tau_{t}}\rho^{\star}_{p}u_{p,II}A_{p}, \quad m^{\star}_{f} = \rho^{\star}_{f}A_{f}L, \tag{41}$$

where it should be noted that A_p and A_f respectively stand for the cross-sectional areas of channels and felt, *for the entire wheel*. Reference values for the thermophysical properties are given by:

$$k^{\star}_{p} = k_{a}, \quad \rho^{\star}_{p} = \rho_{a}, \quad c^{\star}_{p_p} = c_{p_a},$$
$$\rho^{\star}_{f} = (1-\epsilon_{f})\rho_{fs} + \epsilon_{f}\rho_{a}, \tag{42}$$

$$k^{\star}_{f,eff} = (1-\epsilon_{f})k_{fs} + \epsilon_{f}k_{a},$$
$$c^{\star}_{f} = \frac{(1-\epsilon_{f})\rho_{fs}c_{fs} + \epsilon_{f}\rho_{a}c_{p_a}}{\rho^{\star}_{f}}, \tag{43}$$

$$\mathscr{D}^{\star}_{p} = \bar{\mathscr{D}}_{p}, \quad \mathscr{D}^{\star}_{f} = \bar{\mathscr{D}}_{g,eff} + \bar{\mathscr{D}}_{s,eff}. \tag{44}$$

3.2. Dimensionless parameters

The Lewis number is defined for both process stream and sorbent felt as:

$$Le_{p} = \frac{\alpha^{\star}_{p}}{\mathscr{D}^{\star}_{p}}, \quad Le_{f} = \frac{\alpha^{\star}_{f}}{\mathscr{D}^{\star}_{f}}, \quad \text{with}$$
$$\alpha^{\star}_{p} = \frac{k^{\star}_{p}}{\rho^{\star}_{p}c^{\star}_{p_p}}, \quad \alpha^{\star}_{f} = \frac{k^{\star}_{f,eff}}{\rho^{\star}_{f}c^{\star}_{f}}. \tag{45}$$

Biot numbers, for heat and mass transfer, together with Fourier and Fick numbers, defined in terms of the total time of one revolution, are given by:

$$Bi_{h} = \frac{h_{h}\Delta R_{f}}{k^{\star}_{f,eff}}, \quad Bi_{m} = \frac{h_{m}\Delta R_{f}}{\mathscr{D}^{\star}_{f}}, \quad Fo_{t} = \frac{\alpha^{\star}_{f}\tau_{t}}{\Delta R^{2}_{f}},$$
$$Fi_{t} = \frac{\mathscr{D}^{\star}_{f}\tau_{t}}{\Delta R^{2}_{f}}. \tag{46}$$

The psychrometric ratio [27], together with the Nusselt and Sherwood numbers—based on the hydraulic diameter—are given by:

$$\psi_{r} = \frac{h_{h}}{h_{m}\rho^{\star}_{p}c^{\star}_{p_p}}, \quad Nu = \frac{h_{h}D^{H}_{p}}{k^{\star}_{p}}, \quad Sh = \frac{h_{m}D^{H}_{p}}{\mathscr{D}^{\star}_{p}}. \tag{47}$$

As the current study deals with regenerative exchangers, dimensionless parameters that are common in regenerator analyses [26,28] are also employed. The process stream and felt heat capacity rates are given by:

$$C_{I} = (\dot{m}^{\star}_{p}c^{\star}_{p_p})|_{I}, \quad C_{II} = (\dot{m}^{\star}_{p}c^{\star}_{p_p})|_{II}, \quad C_{r,f} = \frac{c^{\star}_{f}m^{\star}_{f}}{\tau_{t}}. \tag{48}$$

In addition, the fluid heat capacity ratio, felt heat capacity ratio, and overall number of sensible heat transfer units are respectively defined as:

$$C^{*} = \frac{C_{min}}{C_{max}}, \quad C^{*}_{r,f} = \frac{C_{r,f}}{C_{min}},$$
$$N^{h}_{tu,o} = \frac{1}{C_{min}}\left[\frac{1}{(h_{h}A_{s})|_{I}} + \frac{1}{(h_{h}A_{s})|_{II}}\right]^{-1}, \tag{49}$$

and the convective conductance ratio is given by:

$$(h_{h}A_{s})^{*} = \frac{(h_{h}A_{s}) \text{ on the } C_{min} \text{ side}}{(h_{h}A_{s}) \text{ on the } C_{max} \text{ side}}. \tag{50}$$

The parameters for mass transfer are similar to the ones defined for heat transfer. Volumetric capacity rates are employed, and these are given by:

$$V_{\mathrm{I}} = \frac{(\dot{m}_{\mathrm{a}})|_{\mathrm{I}}}{\rho_{\mathrm{a}}}, \quad V_{\mathrm{II}} = \frac{(\dot{m}_{\mathrm{a}})|_{\mathrm{II}}}{\rho_{\mathrm{a}}}, \quad V_{\mathrm{r,f}} = \frac{A_{\mathrm{f}} L}{\tau_{\mathrm{t}}}. \tag{51}$$

Based on the previous definitions, volumetric capacity ratios and the overall number of mass transfer units are also defined:

$$V^* = \frac{V_{\min}}{V_{\max}}, \quad V^*_{\mathrm{r,f}} = \frac{V_{\mathrm{r,f}}}{V_{\min}},$$
$$N^{\mathrm{m}}_{\mathrm{tu,o}} = \frac{1}{V_{\min}} \left[\frac{1}{(h_{\mathrm{m}} A_{\mathrm{s}})|_{\mathrm{I}}} + \frac{1}{(h_{\mathrm{m}} A_{\mathrm{s}})|_{\mathrm{II}}} \right]^{-1}. \tag{52}$$

Finally, the *convective* "*mass-conductance*" *ratio* is defined:

$$(h_{\mathrm{m}} A_{\mathrm{s}})^* = \frac{(h_{\mathrm{m}} A_{\mathrm{s}}) \text{ on the } V_{\min} \text{ side}}{(h_{\mathrm{m}} A_{\mathrm{s}}) \text{ on the } V_{\max} \text{ side}}. \tag{53}$$

Since h_{h} and h_{m} are constants, the individual surface and cross-sectional areas are equal for all channels, and considering the case with $u_{\mathrm{p,I}} = u_{\mathrm{p,II}}$, the previous parameters are shown to be related through the following expressions:

$$C^* = V^* = (h_{\mathrm{h}} A_{\mathrm{s}})^* = (h_{\mathrm{m}} A_{\mathrm{s}})^* = \frac{\tau_{\min}}{\tau_{\max}}, \tag{54}$$

$$Fi_{\mathrm{t}} = \frac{(1+V^*)^2}{V^*} \frac{K_{\mathrm{r}} N^{\mathrm{m}}_{\mathrm{tu,o}}}{Bi_{\mathrm{m}} V^*_{\mathrm{r,f}}},$$
$$Fo_{\mathrm{t}} = \frac{(1+C^*)^2}{C^*} \frac{K_{\mathrm{r}} N^{\mathrm{h}}_{\mathrm{tu,o}}}{Bi_{\mathrm{h}} C^*_{\mathrm{r,f}}}, \quad \text{with} \quad K_{\mathrm{r}} = \frac{A_{\mathrm{f}}}{P_{\mathrm{p}} \Delta R_{\mathrm{f}}}, \tag{55}$$

$$Le_{\mathrm{f}} = \frac{Fo_{\mathrm{t}}}{Fi_{\mathrm{t}}}, \quad C^*_{\mathrm{r,f}} = \frac{c^{\star}_{\mathrm{f}} \rho^{\star}_{\mathrm{f}}}{c^{\star}_{p_{\mathrm{p}}} \rho^{\star}_{\mathrm{p}}} V^*_{\mathrm{r,f}}, \quad \psi_{\mathrm{r}} = \frac{N^{\mathrm{h}}_{\mathrm{tu,o}}}{N^{\mathrm{m}}_{\mathrm{tu,o}}} = Le_{\mathrm{p}} \frac{Nu}{Sh}, \tag{56}$$

where $\tau_{\min}$ and $\tau_{\max}$ are the minimum and maximum values of τ_{I} and τ_{II}, and the parameter K_{r} basically depends on the curvature of the felt. If the effects of such curvature are negligible, $K_{\mathrm{r}} \approx 1$.

The ratio between the number of transfer units for heat and mass transfer in Eq. (56) is similar to that presented in [12,29]; however, in those studies, the psychrometric ratio is termed the Lewis number. Although this terminology is common among several investigations, in this treatise, Lewis numbers are defined through Eq. (45), being only fluid-dependent.

3.3. Dimensionless governing equations

The governing differential equations and boundary conditions are fully normalized by introducing the following dimensionless variables and operators:

$$x^* = \frac{x}{L}, \quad r^* = \frac{r - R_{\mathrm{p}}}{\Delta R_{\mathrm{f}}}, \quad t^* = \frac{t}{\tau_{\mathrm{t}}}, \quad \nabla_* = \Delta R_{\mathrm{f}} \nabla, \tag{57}$$

$$\Theta_{\mathrm{p}} = \frac{T_{\mathrm{p}} - T_{\mathrm{ref}}}{\Delta T_{\mathrm{ref}}}, \quad \Theta_{\mathrm{f}} = \frac{T_{\mathrm{f}} - T_{\mathrm{ref}}}{\Delta T_{\mathrm{ref}}}, \tag{58}$$

$$\Phi_{\mathrm{p}} = \frac{Y_{\mathrm{p}} - Y_{\mathrm{ref}}}{\Delta Y_{\mathrm{ref}}}, \quad \Phi_{\mathrm{fp}} = \frac{Y_{\mathrm{fp}} - Y_{\mathrm{ref}}}{\Delta Y_{\mathrm{ref}}}, \quad \Phi_{\mathrm{fm}} = \frac{W_{\mathrm{fm}}}{W^{\max}_{\mathrm{fm}}}. \tag{59}$$

Substituting the previous relations in Eqs. (20), (21), (30) and (31), yields:

$$\frac{1}{Fi_{\mathrm{t}}} \left((1-\epsilon_{\mathrm{f}}) f_{\mathrm{s}} \Omega_{\max} \frac{\partial \Phi_{\mathrm{fm}}}{\partial t^*} + \epsilon_{\mathrm{f}} \frac{\partial \Phi_{\mathrm{fp}}}{\partial t^*} \right) = f_{\mathrm{s}} \Omega_{\max} \nabla_* \cdot (\delta_{\mathrm{s}} \nabla_* \Phi_{\mathrm{fm}}) + \nabla_* \cdot (\delta_{\mathrm{g}} \nabla_* \Phi_{\mathrm{fp}}), \tag{60}$$

$$\frac{\chi_{\mathrm{f}}}{Fo_{\mathrm{t}}} \frac{\partial \Theta_{\mathrm{f}}}{\partial t^*} = \nabla_* \cdot (\kappa_{\mathrm{f}} \nabla_* \Theta_{\mathrm{f}}) + \frac{\varphi_{\mathrm{sor}} f_{\mathrm{s}} \Omega_{\max}}{Le_{\mathrm{f}}} \times \left(\frac{1}{Fi_{\mathrm{t}}} (1-\epsilon_{\mathrm{f}}) \frac{\partial \Phi_{\mathrm{fm}}}{\partial t^*} - \nabla_* \cdot (\delta_{\mathrm{s}} \nabla_* \Phi_{\mathrm{fm}}) \right), \tag{61}$$

$$\tau^*_{\mathrm{dw}} \frac{\mathrm{D}\Phi_{\mathrm{p}}}{\mathrm{D}t^*} = (1+V^*) N^{\mathrm{m}}_{\mathrm{tu,o}} (\Phi_{\mathrm{fp}}|_{\mathrm{p.s.}} - \Phi_{\mathrm{p}}), \tag{62}$$

$$\chi_{\mathrm{p}} \tau^*_{\mathrm{dw}} \frac{\mathrm{D}\Theta_{\mathrm{p}}}{\mathrm{D}t^*} = (1+C^*) N^{\mathrm{h}}_{\mathrm{tu,o}} (\Theta_{\mathrm{f}}|_{\mathrm{p.s.}} - \Theta_{\mathrm{p}}), \tag{63}$$

where the dimensionless material derivative is given in terms of the dimensionless dwell time:

$$\frac{\mathrm{D}}{\mathrm{D}t^*} = \frac{\partial}{\partial t^*} + \frac{1}{\tau^*_{\mathrm{dw}}} \frac{\partial}{\partial x^*}, \quad \text{with} \quad \tau^*_{\mathrm{dw}} = \frac{\tau_{\mathrm{dw}}}{\tau_{\mathrm{t}}} = \frac{L}{u_{\mathrm{p}} \tau_{\mathrm{t}}}. \tag{64}$$

At the interface $r^* = 0$, the following boundary conditions apply:

$$-f_{\mathrm{s}} \Omega_{\max} \delta_{\mathrm{s}} \frac{\partial \Phi_{\mathrm{fm}}}{\partial r^*} - \delta_{\mathrm{g}} \frac{\partial \Phi_{\mathrm{fp}}}{\partial r^*} = Bi_{\mathrm{m}} (\Phi_{\mathrm{p}} - \Phi_{\mathrm{fp}}), \tag{65}$$

$$-\kappa_{\mathrm{f}} \frac{\partial \Theta_{\mathrm{f}}}{\partial r^*} = Bi_{\mathrm{h}} (\Theta_{\mathrm{p}} - \Theta_{\mathrm{f}}) + \frac{Bi_{\mathrm{m}}}{Le_{\mathrm{f}}} (\Phi_{\mathrm{p}} - \Phi_{\mathrm{fp}}) \varphi_{\mathrm{v},\Delta T} - \frac{f_{\mathrm{s}} \Omega_{\max}}{Le_{\mathrm{f}}} \delta_{\mathrm{s}} \frac{\partial \Phi_{\mathrm{fm}}}{\partial r^*} \varphi_{\mathrm{sor}}, \tag{66}$$

whereas at the other boundaries one finds:

$$\left(\frac{\partial \Phi_{\mathrm{fp}}}{\partial r^*} \right)_{r^*=1} = \left(\frac{\partial \Theta_{\mathrm{f}}}{\partial r^*} \right)_{r^*=1} = 0,$$
$$\left(\frac{\partial \Phi_{\mathrm{fp}}}{\partial x^*} \right)_{x^*=0} = \left(\frac{\partial \Theta_{\mathrm{f}}}{\partial x^*} \right)_{x^*=0} = 0,$$
$$\left(\frac{\partial \Phi_{\mathrm{fp}}}{\partial x^*} \right)_{x^*=1} = \left(\frac{\partial \Theta_{\mathrm{f}}}{\partial x^*} \right)_{x^*=1} = 0. \tag{67}$$

The normalized periodic inlet conditions are given by:

$$\left.\begin{aligned} &\Phi_{\mathrm{p}}(0,t^*) = \Phi^{\mathrm{I}}_{\mathrm{in}}(t^*), \quad \Theta_{\mathrm{p}}(0,t^*) = \Theta^{\mathrm{I}}_{\mathrm{in}}(t^*), \\ &\quad \text{for} \quad 0 \leqslant t^* \leqslant \tfrac{\tau_{\mathrm{I}}}{\tau_{\mathrm{t}}} \\ &\Phi_{\mathrm{p}}(0,t^*) = \Phi^{\mathrm{II}}_{\mathrm{in}}(t^*), \quad \Theta_{\mathrm{p}}(0,t^*) = \Theta^{\mathrm{II}}_{\mathrm{in}}(t^*), \\ &\quad \text{for} \quad \tfrac{\tau_{\mathrm{I}}}{\tau_{\mathrm{t}}} \leqslant t^* \leqslant 1 \end{aligned}\right\} \quad \text{for} \quad N = 1, 2, \ldots, \tag{68}$$

where N corresponds to the number of revolutions, and—in each of these—the dimensionless process time t^* varies from 0 to 1. In addition, the change of variable

$$x^*_{\text{next}} = 1 - x^*_{\text{current}}, \tag{69}$$

should be applied at the end of each process for obtaining a counterflow configuration.

Finally, the local equilibrium relation is expressed in dimensionless form as:

$$\Phi_{\text{fm}} = \Phi_{\text{fm}}(\Theta_{\text{f}}, \Phi_{\text{fp}}). \tag{70}$$

The additional symbols that appear in Eqs. (60)–(63) are the dimensionless forms of the heat of sorption, heat of sorbate transfer at the interface, and maximum sorbate uptake:

$$\varphi_{\text{sor}} = \frac{i_{\text{sor}}\rho_{\text{a}}\Delta Y_{\text{ref}}}{c^\star_{\text{f}}\rho^\star_{\text{f}}\Delta T_{\text{ref}}}, \quad \varphi_{\text{v},\Delta T} = \frac{i_{\text{v},\Delta T}\rho_{\text{a}}\Delta Y_{\text{ref}}}{c^\star_{\text{f}}\rho^\star_{\text{f}}\Delta T_{\text{ref}}},$$
$$\Omega_{\max} = \frac{\rho_{\text{fs}} W^{\max}_{\text{fm}}}{\rho_{\text{a}}\Delta Y_{\text{ref}}}, \tag{71}$$

and the dimensionless coefficients that include the variable physical properties:

$$\kappa_{\text{f}} = \frac{k_{\text{f,eff}}}{k^\star_{\text{f,eff}}}, \quad \delta_{\text{g}} = \frac{\mathscr{D}_{\text{g,eff}}}{\mathscr{D}^\star_{\text{f}}}, \quad \delta_{\text{s}} = \frac{\mathscr{D}_{\text{s,eff}}}{\mathscr{D}^\star_{\text{f}}},$$
$$\chi_{\text{p}} = \frac{c_{p_{\text{p}}}\rho_{\text{p}}}{c^\star_{p_{\text{p}}}\rho^\star_{\text{p}}}, \quad \chi_{\text{f}} = \frac{c_{\text{f}}\rho_{\text{f}}}{c^\star_{\text{f}}\rho^\star_{\text{f}}}. \tag{72}$$

It should be mentioned, that a single characteristic length was used to normalize the Del operator, implying that the normalized gradient operator inherently includes aspect ratios between the characteristic dimensions employed. For instance, in a two-dimensional configuration with a Cartesian coordinate system one finds:

$$\nabla_* = \left(K_{\text{f}}\frac{\partial}{\partial x^*}, \frac{\partial}{\partial r^*}\right), \quad \text{with} \quad K_{\text{f}} = \frac{\Delta R_{\text{f}}}{L}. \tag{73}$$

By observing the dimensionless parameters and governing equations, one notices that twelve characteristic dimensionless parameters are required for describing the current problem. These include usual parameters for regenerative exchangers ($N^{\text{h}}_{\text{tu,o}}$, $N^{\text{m}}_{\text{tu,o}}$, $V^*_{\text{r,f}}$, $C^*_{\text{r,f}}$, C^*, and τ^*_{dw}), parameters resulting from considering conduction and diffusion in the felt (Bi_{h}, Bi_{m}, and K_{f}), and extra parameters due to adsorption being present ($f_{\text{s}}\Omega_{\max}$ and φ_{sor}). One should also mention $\varphi_{\text{v},\Delta T}$, which is due to coupled heat and mass transfer to the felt. Furthermore, the parameters Fi_{t}, Fo_{t}, V^*, $(h_{\text{m}}A_{\text{s}})^*$ and $(h_{\text{h}}A_{\text{s}})^*$ have been omitted because they depend on others.

The groupings $f_{\text{s}}\Omega_{\max}$, φ_{sor} and $\varphi_{\text{v},\Delta T}$ reflect the problem dependence on the operational conditions due to the coupled nature of the transfer processes, since they explicitly involve the reference temperatures and humidity ratios. Naturally, some of the dimensionless coefficients (72) may also contribute to this dependence, because of their non-linear character.

Once the governing equations and boundary conditions are written in the presented dimensionless form, in which physically meaningful characteristic parameters are employed, the analysis becomes much clearer. As a result, one can examine the order-of-magnitude of terms in the governing equations to provide a qualitative indication of possible simplifications to the equations. For instance, the storage term in the process stream equations—which represent the *process stream carry-over*—becomes negligible for $\tau^*_{\text{dw}} \ll 1$, which indeed occurs in slower desiccant wheels, but not in enthalpy exchangers. Furthermore, the gas-phase storage term in Eq. (60) would be insignificant if $f_{\text{s}}\Omega_{\max}$ is large and $\epsilon_{\text{f}} \ll 1$. Another term that is a potential candidate for elimination is that involving the enthalpy change due to mass transfer to the felt, in Eq. (60), provided that $\varphi_{\text{v},\Delta T} \approx 0$. This is generally true for normal operation condition with moist air, and an exception are cases in which $|\Delta Y_{\text{ref}}/\Delta T_{\text{ref}}| > 1$, or if the sorbate is such that $i_{\text{v},\Delta T}$ is large. Regarding the axial conduction and mass diffusion within the felt, knowing beforehand that K_{f} is small and that the felt has isotropic properties does not readily justify discarding these terms, since gradients can be much higher in the axial direction, and especially because these terms involve second derivatives. The effect of neglecting these terms should be further investigated; however, a numerical investigation that addresses these questions is out of this scope of this study. Hence, all results presented in this work are evaluated preserving all terms in the governing equations.

By comparing governing equations and boundary conditions included in different mathematical formulations, it was observed that all terms that contribute to heat and mass transfer within the felt and between the felt and process stream contained in previously published studies are included in the current model. Furthermore, the current formulation includes extra terms, which are associated with additional transport rates that were not accounted for in previous investigations. These terms could eventually be eliminated, once additional simplifying assumptions are considered.

4. Results

This section presents results obtained with the provided dimensionless mathematical formulation, which was solved using a numerical algorithm based on the finite volumes method. At first, comparative results, using data from previous studies—including experimental measurements—are presented for validating the formulation. Then, simulation results of a test-case, consisting of heat and mass transfer in an enthalpy wheel, are analyzed.

All results were calculated considering moist air as the solvent-sorbate pair, the properties of which are listed in Table 1. This table also includes the data for all properties and geometry employed in the simulations. In addition, the expressions for sorbate diffusivity and thermal conductivity are described next.

In the gas-phase of the felt, ordinary molecular diffusion, Knudsen diffusion, or an intermediate regime with both phenomena can occur, and an approximate expression that accounts for all these configurations [30] is employed:

$$\frac{1}{\mathscr{D}_g} = \frac{1}{\mathscr{D}_M} + \frac{1}{\mathscr{D}_K}. \tag{74}$$

For both molecular and Knudsen diffusivities, Fick's-law type expressions are readily found in literature [31]. For air-water vapor mixtures these expressions reduce to:

$$\mathscr{D}_M = 1.735 \times 10^{-9} \frac{T^{1.685}}{P}, \quad \mathscr{D}_K = 97 v_r \sqrt{\frac{T}{18.015}}, \tag{75}$$

where P should be given in atmospheres, T in Kelvin, and v_r in meters. For surface diffusivity, the formula proposed in [24,32] is employed:

$$\mathscr{D}_s = \mathscr{D}_0 \exp\left(-\alpha_s \frac{i_{sor}}{RT}\right), \tag{76}$$

where the constants $\mathscr{D}_0$ and α_s can be found in Table 1. For the thermal conductivities k_{pd} and k_{fm}, mass-weighted averages are employed, for simplicity:

$$k_{fp} = \frac{\rho_a k_a + k_v Y_{fp}}{\rho_a (1 + Y_{fp})}, \quad k_{fm} = \frac{\rho_{fs} k_{fs} + k_l f_s W_{fm}}{\rho_{fs}(1 + f_s W_{fm})}, \tag{77}$$

The performance of the rotary regenerator is assessed by means of effectiveness. Since the three major quantities in the current problem are temperature, mass concentration and enthalpy, an effectiveness is defined for each of these:

$$\varepsilon_t = \frac{\tau_I}{\tau_{min}} \frac{(\bar{\Theta}^{out}_{p,I} - \Theta^{in}_{p,I})}{(\Theta^{in}_{p,II} - \Theta^{in}_{p,I})}, \quad \varepsilon_m = \frac{\tau_I}{\tau_{min}} \frac{\bar{\Phi}^{out}_{p,I} - \Phi^{in}_{p,I}}{\Phi^{in}_{p,II} - \Phi^{in}_{p,I}},$$
$$\varepsilon_i = \frac{\tau_I}{\tau_{min}} \frac{\bar{\tilde{i}}^{out}_{p,I} - \tilde{i}^{in}_{p,I}}{\tilde{i}^{in}_{p,II} - \tilde{i}^{in}_{p,I}}, \tag{78}$$

where,

$$\bar{\Theta}^{out}_{p,I} = \frac{1}{\tau_I} \int_0^{\tau_I} \Theta^{out}_{p,I}\, dt^*,$$
$$\bar{\Phi}^{out}_{p,I} = \frac{1}{\tau_I} \int_0^{\tau_I} \Phi^{out}_{p,I}\, dt^*, \quad \bar{\tilde{i}}^{out}_{p,I} = \frac{1}{\tau_I} \int_0^{\tau_I} \tilde{i}^{out}_{p,I}\, dt^*, \tag{79}$$

and the enthalpies are calculated using Eq. (9). Also, the values of specific enthalpies of individual components, required in some calculations, are given by the following expressions:

$$i_a(T) = i^0_a + c_{pa}(T - T^0),$$
$$i_v(T) = i^0_v + c_{pv}(T - T^0), \tag{80}$$
$$i_{ls}(T) = i^0_{ls} + c_{ls}(T - T^0),$$
$$i_{fs}(T) = i^0_{fs} + c_{fs}(T - T^0), \tag{81}$$

where the zero superscripts denote reference values at T^0, which is chosen as 0 °C. Additionally, the heat of vaporization is directly calculated by $i_{vap} = i_v - i_{ls}$.

Table 1
Input data used in simulations

Common input data					
c_{pa}	1007 J/kg °C	k_a	26.3×10^{-3} W/m °C	ρ_a	1.1614 kg/m^3
c_{pv}	1872 J/kg °C	k_v	19.6×10^{-3} W/m °C	$\mathscr{D}^{\star}_p$	2.94×10^{-5} m^2/s
c_{ls}	4180 J/kg °C	k_l	613×10^{-3} W/m °C	$\mathscr{D}^{\star}_f$	3.43×10^{-6} m^2/s
ϵ_f	0.30	α_s	0.45	$\mathscr{D}_0$	1.6×10^{-6} m^2/s
τ_g	3.0	τ_s	3.0	$2v_r$	1.0 μm
Experimental validation input data					
ρ_{fs}	930 kg/m^3	k_{fs}	0.011 W/m °C	c_{fs}	1340 J/kg °C
W^{max}_{fm}	0.234 kg/kg	β	0.748	L	202.3 mm
$2a$	1.5 mm	$2b$	3.0 mm	$2\Delta R_f$	0.25 mm
T^{I}_{in}	34.5 °C	T^{II}_{in}	120 °C	Nu	2.135
Y^{I}_{in}	14.5 g/kg	Y^{II}_{in}	18.5 g/kg	u_{face}	1.5 m/s
Test-case input data					
T^{I}_{in}	30 °C	T^{II}_{in}	15 °C	ρ_{fs}	800 kg/m^3
ϕ^{I}_{in}	40%	ϕ^{II}_{in}	40%	c_{fs}	920 J/kg °C
C^*	1.0	K_f	0.001	W^{max}_{fm}	0.40 kg/kg
Bi_h	0.1	$N^{h}_{tu,o}$	3.5	$C^{*}_{r,f}$	$20/\tau_t$
Bi_m	4.0	$N^{m}_{tu,o}$	4.0	τ^{*}_{dw}	$0.08/\tau_t$

4.1. Validation of formulation

In order to validate the current mathematical model, initially, simulated effectiveness results for a sensible heat transfer regenerator are compared to those presented by Kays and London [28]. Table 2 displays the enthalpy effectiveness, which in this case is identical to the temperature effectiveness, together with selected cases for periodic-flow exchangers from [28]. These periodic simulations were calculated with a 20×5 grid, considering $\Phi^{in}_{p,I}=\Phi^{in}_{p,II}=0$, $\Theta^{in}_{p,I}=1$ and $\Theta^{in}_{p,II}=0$, using the following values as input data: $C^*=1$, $N^m_{tu,o}=1$, $f_s\Omega_{max}=0$, $\tau^*_{dw}=10^{-5}$, and $Bi_m=Bi_h=0.001$. The dimensionless dwell time and the Biot numbers were set to small values, since carry-over effects and diffusion in the matrix, for the compared cases, are omitted in [28]. By observing Table 2, one notices very good agreement between the current results and the ones presented by Kays and London [28].

In addition to the previous validation, data from the current formulation are compared with that experimentally obtained by Brillhart [33], which were obtained from measurements of periodic heat and mass transfer in a desiccant sample, which consisted of a corrugated paper matrix coated with sorbent material. The cross section view of this sample, provided in [33], indicates that the geometry of the channels can be represented by a sine-curved top and a flat base, which is characterized by three parameters: channel base ($2b$), channel height ($2a$) and channel wall thickness ($2\Delta R_f$). Despite the sample presents considerable deviation in size among its channels, representative values for ($2b$), ($2a$) and ($2\Delta R_f$) were obtained, all of which are given in Table 1. For the Nusselt number, the value obtained for sinusoidal channels with $b/a=2$ [34], also displayed in Table 1, was employed. Using the Nusselt number, Sh was calculated from Eq. (56), in which the value for the psychrometric ratio is obtained from [35]. One should also mention that, given the geometry of the channels, the velocity u_p was calculated from the face velocity u_{face} and the open area fraction, which is directly obtained from the geometry.

The equilibrium relation for this desiccant is given by $f_sW_{fm}=W^{max}_{fm}\phi^{\beta}_{fp}$, where the constants W^{max}_{fm} and β are also presented in Table 1. For the heat of sorption and remaining thermo-physical properties of the tested sample were unavailable in [33]. However, since the sample consisted of paper coated with sorbent, the thermo-physical properties of paper were used for simulating the tested material. In addition, since the heat of sorption is commonly about 20% over the value of the heat of vaporization, the following expressions were used to determine the value of i_{sor} and i_{wet}:

$$i_{sor}=(1+e_{sor})i_{vap},\quad i_{wet}=-e_{sor}i_{vap},\quad \text{with}\quad e_{sor}=0.20. \tag{82}$$

Fig. 2 shows temperature and humidity ratio profiles obtained with the current formulation, together with those measured by [33]. As one can observe, despite the lack of data, the simulation results present a very reasonable agreement with the experimental ones, with higher discrepancies occurring for the Y_p curves at the initial region of period I. Nevertheless, the experimental uncertainties are always elevated in the beginning of an adsorption period, which thereby justifies the high discrepancy obtained in that portion of the cycle.

Besides the previous validation results, integral mass and energy balances between the process stream and sorbent felt were performed, and in all cases—including the test-case results in the next section—the relative error was inferior to 10^{-3}.

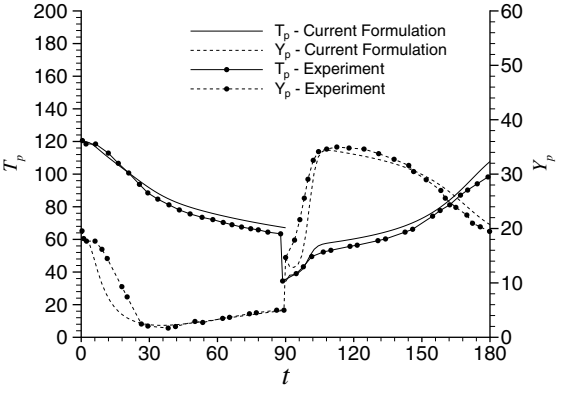

Fig. 2. Experimental validation: outlet values of temperature T_p and concentration Y_p with time t.

Table 2
Comparison with effectiveness for heat transfer regenerator

$N^h_{tu,o}$	$C^*_{r,f}=1.0$		$C^*_{r,f}=2.0$	
	Ref. [28]	Current	Ref. [28]	Current
2.0	0.601	0.6009	0.649	0.6491
3.0	0.667	0.6673	0.728	0.7280
4.0	0.709	0.7088	0.776	0.7760
5.0	0.738	0.7377	0.809	0.8085

4.2. Test-case

To illustrate the proposed formulation, simulation results of a test-case, comprising heat and mass transfer in a selected enthalpy wheel, are presented. The results involve an investigation of the impact of varying sorbent mass fraction in the matrix and wheel rotational speed. The input data used in the simulations can be found in Table 1, and the equilibrium relation $W_{fm} = W_{fm}^{max}\phi_{dp}$ was employed. For the heat of sorption, the same expression used in the experimental validation was adopted.

In order to obtain insight on the sorption phenomena in the sorbent material, the evolution of the sorbate distribution in the matrix with the dimensionless time was locally examined. Fig. 3 provides contour plots of Φ_{fm} for $t^* = 0$, 0.25, 0.5, and 0.75, for a rotor operating at 60 RPM with the inlet values described in Table 1. As can be seen, the matrix uptakes sorbate during period I and releases sorbate in period II; however, this reversible sorbate-motion mostly occurs within the upper half of the felt, which suggests—if Θ_f and Φ_{fp} also present little dependence in r within the lower portion of the felt—that the felt thickness could be reduced without degrading regenerator performance. Analyzing the dimensionless temperature and gas-phase concentration contour plots (Fig. 4) reveals that those potentials are less dependent on r^* (especially Θ_f) than Φ_{fm} is and that most of the temperature and concentration gradients indeed occur at the upper portion of the felt.

The effect of varying sorbent mass fraction and process time on the performance results is illustrated in Fig. 5. As displayed, in general, the ε's decrease with τ_t and increase with f_s; also, for the presented cases, the mass transfer effectiveness is always lower than the enthalpy effectiveness. Furthermore, the mass and enthalpy effectiveness present a steep fall within the lower values of τ_t. This decrease tends to be less severe as f_s is

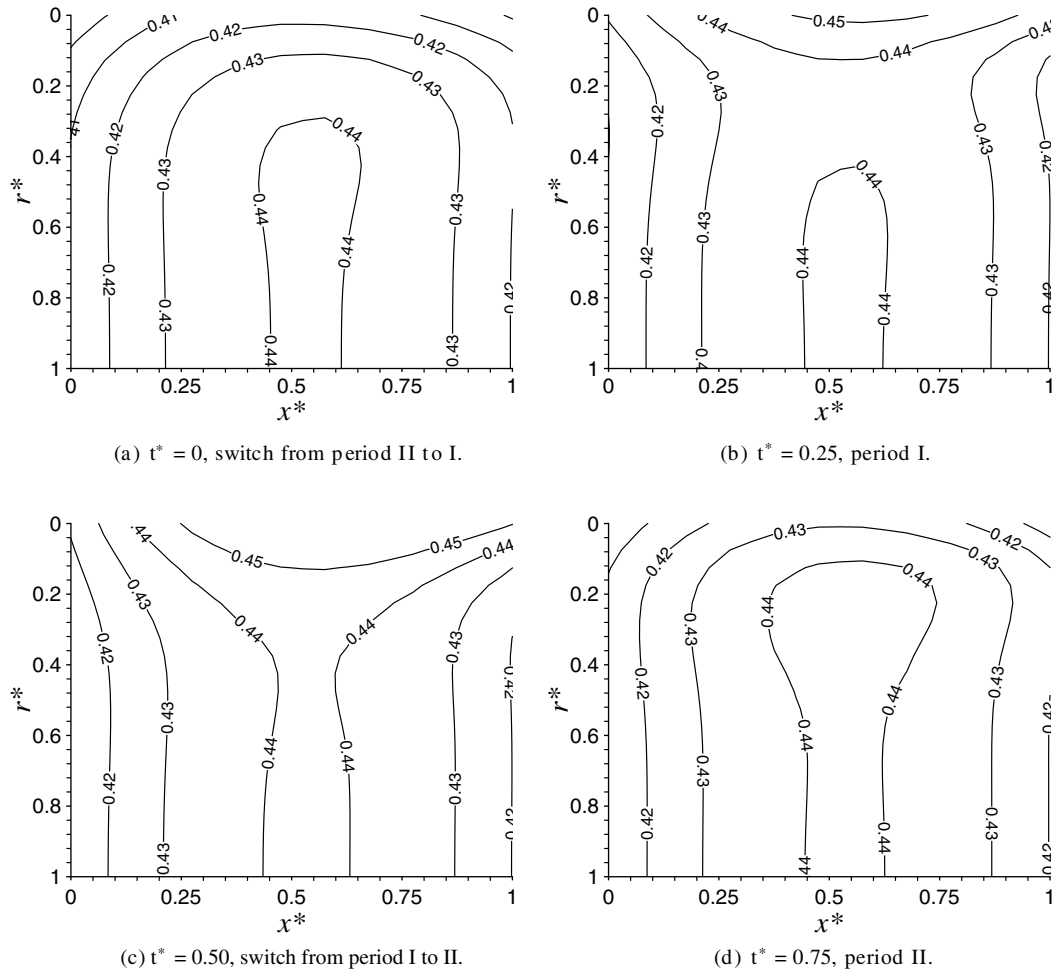

(a) $t^* = 0$, switch from period II to I.

(b) $t^* = 0.25$, period I.

(c) $t^* = 0.50$, switch from period I to II.

(d) $t^* = 0.75$, period II.

Fig. 3. Contour plots of $\Phi_{fm}(x^*, r^*, t^*)$ for test-case with $f_s = 0.10$ and $\tau_t = 1$ s, at four different dimensionless times t^*.

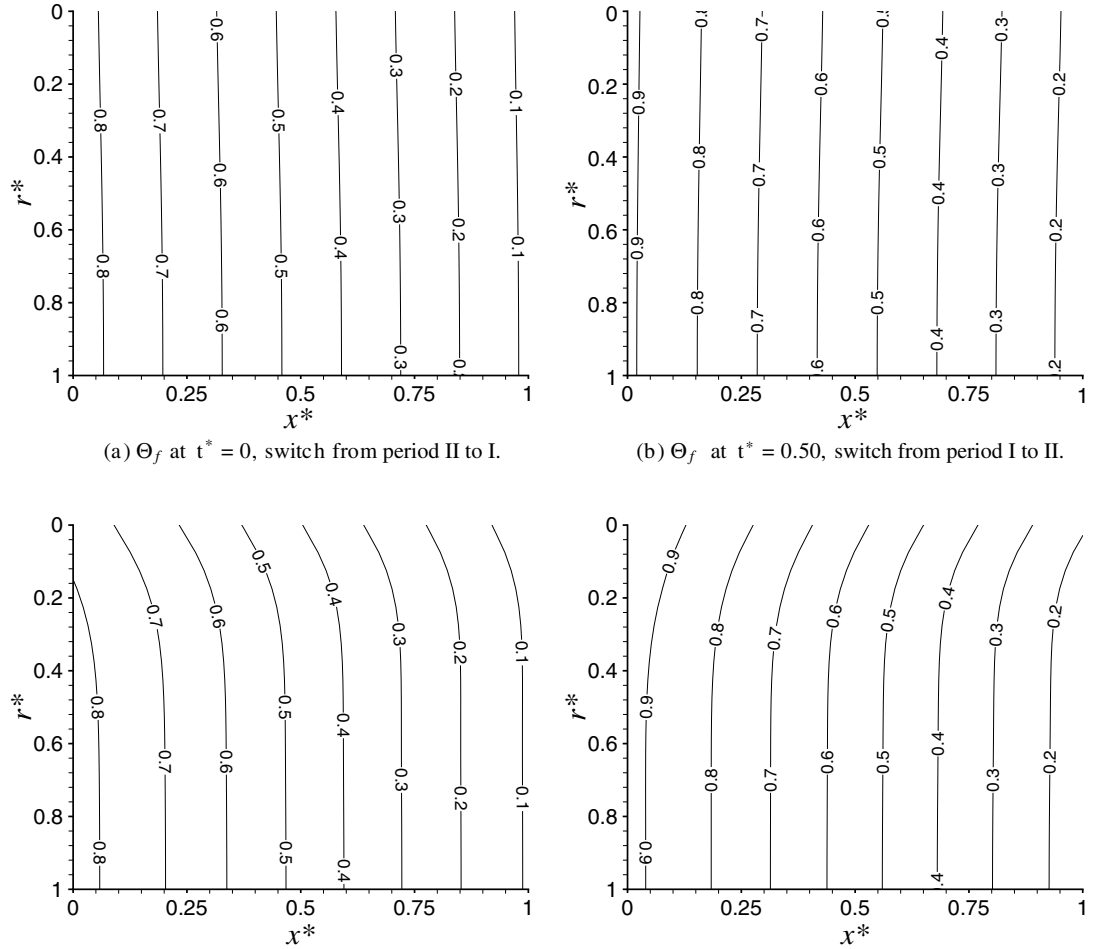

(a) Θ_f at $t^* = 0$, switch from period II to I.

(b) Θ_f at $t^* = 0.50$, switch from period I to II.

(c) Φ_{fp} at $t^* = 0$, switch from period II to I.

(d) Φ_{fp} at $t^* = 0.50$, switch from period I to II.

Fig. 4. Contour plots of $\Theta_f(x^*, r^*, t^*)$ and $\Phi_{fp}(x^*, r^*, t^*)$ for test-case with $f_s = 0.10$ and $\tau_t = 1$ s, at two different dimensionless times t^*.

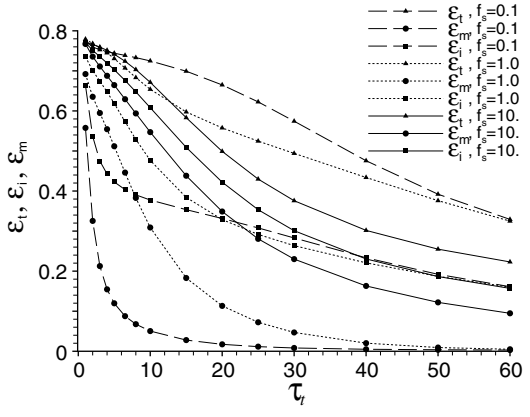

Fig. 5. Variation of effectiveness ε's in test-case with the process time τ_t for different values of sorbent mass fraction f_s.

increased. In addition, this figure demonstrates the inappropriateness of using ε_t instead of ε_i for assessing the performance of an enthalpy wheel. Nevertheless, it is interesting to note that ε_i appears to be an average of ε_t and ε_m. As one can also observe, the differences between ε_i and ε_m are much more pronounced for lower f_s's. In addition, this figure also seems to suggest that ε_i becomes weakly dependent of f_s as τ_t approaches 60 s.

5. Summary and conclusions

A new mathematical model for the transfer processes involved in adsorption-based regenerative heat and mass exchangers was formally developed, with efforts aimed on a detailed description of the transport phenomena occurring within the porous sorbent felt. A thorough discussion of the relevant dimensionless groups was

performed, and a fully normalized system of governing partial differential equations was obtained. These equations include all terms due to transfer within the sorbent felt and between the felt and process stream considered in previous studies.

A simulation of a test-case was conducted, showing that the performance generally increases with f_s and decreases with τ_t, and suggesting a possibility of optimizing construction costs and compactness by reducing the amount of required felt material. Therefore, a more detailed examination of the impact of varying felt thickness should be performed. Finally, as this investigation was focused on establishing a mathematical formulation and determining relevant dimensionless parameters, there is a clear need for further research regarding the influence of the characteristic parameters on regenerator performance.

Regardless of the necessity for further investigation, the proposed formulation is general, as it can be used for simulating both enthalpy and desiccant wheels, accurate, since it was validated against previous studies—including experimental data, and versatile, as it can be easily adapted to incorporate additional features—such as including a supporting structure, considering entrance regions, and employing additional temperature-dependent properties.

Acknowledgements

The authors would like to acknowledge the financial support provided by, CNPq (Brazil) and the University of Illinois at Chicago.

References

[1] D. Roy, D. Gidaspow, Nonlinear coupled heat and mass exchange in a cross-flow regenerator, Chem. Eng. Sci. 29 (1974) 2101–2114.
[2] B. Mathiprakasam, Z. Lavan, Performance predictions for adiabatic desiccant dehumidifiers using linear solutions, J. Solar Energy Eng. (Trans. ASME) 102 (1980) 73–79.
[3] V.C. Mei, Z. Lavan, Performance of crossed-cooled desiccant dehumidifiers, J. Solar Energy Eng. (Trans. ASME) 105 (1983) 300–304.
[4] J.J. Jurinak, J.W. Mitchell, Effect of matrix properties on the performance of a counterflow rotary dehumidifier, J. Heat Transfer (Trans. ASME) 106 (1984) 638–645.
[5] D. Charoensupaya, W.M. Worek, Parametric study of an open-cycle adiabatic, solid, desiccant cooling system, Energy 13 (9) (1988) 739–747.
[6] D. Charoensupaya, W.M. Worek, Effect of adsorbent heat and mass transfer resistances on performance of an open-cycle adiabatic desiccant cooling system, Heat Recovery Syst. CHP 8 (6) (1988) 537–548.
[7] P. Majumdar, W.M. Worek, Combined heat and mass transfer in a porous adsorbent, Energy 14 (3) (1989) 161–175.
[8] W. Zheng, W.M. Worek, Numerical simulation of combined heat and mass transfer processes in rotary dehumidifier, Num. Heat Transfer, Part A 23 (1993) 211–232.
[9] P. Majumdar, Heat and mass transfer in composite pore structures for dehumidification, Solar Energy 62 (1) (1998) 1–10.
[10] H. Klein, S.A. Klein, J.W. Mitchell, Analysis of regenerative enthalpy exchangers, Int. J. Heat Mass Transfer 33 (4) (1990) 735–744.
[11] C.J. Simonson, R.W. Besant, Heat and moisture transfer in dessicant coated rotary energy exchangers: Part I. numerical model, HVAC R Res. 3 (4) (1997) 325–350.
[12] G. Stiesch, S.A. Klein, J.W. Mitchell, Performance of rotary heat and mass exchangers, HVAC R Res. 1 (4) (1995) 308–323.
[13] C.J. Simonson, R.W. Besant, Energy wheel effectiviness. Part I: Development of dimensionless groups, Int. J. Heat Mass Transfer 42 (1999) 2161–2170.
[14] I.L. Maclaine-Cross, P.J. Banks, Coupled heat and mass transfer in regenerators—predictions using an analogy with heat transfer, Int. J. Heat Mass Transfer 15 (1972) 1225–1242.
[15] R.B. Holmberg, Combined heat and mass transfer in regenerators with hygroscopic materials, J. Heat Transfer—Trans. ASME 101 (1979) 205–210.
[16] P.J. Banks, Prediction of heat and mass regenerator performance using nonlinear analogy method. Part I: Basis, J. Heat Transfer (Trans. ASME) 107 (1985) 222–229.
[17] E. Van den Bulck, J.W. Mitchell, S.A. Klein, Design theory for rotary heat and mass exchangers. I: Wave analysis of rotary heat and mass exchangers with infinite transfer coefficients, Int. J. Heat Mass Transfer 28 (8) (1985) 1575–1586.
[18] J.L. Niu, L.Z. Zhang, Effects of wall thickness on the heat and moisture transfers in desiccant wheels for air dehumidification and enthalpy recovery, Int. Commun. Heat Mass Transfer 29 (2) (2002) 255–268.
[19] J.L. Niu, L.Z. Zhang, Performance comparisons of desiccant of desiccant wheels for air dehumidification and enthalpy recovery, Appl. Therm. Eng. 22 (2002) 1347–1367.
[20] B. Jacob, Dynamics of fluids in porous media, Dover, Mineola, NY, 1988, Reprint, originally published by American Elsevier Pub. Co., 1972.
[21] M. Kaviany, Principles of Heat Transfer in Porous Media, second ed., Springer-Verlag, New York, NY, 1995.
[22] D.J. Close, P.J. Banks, Coupled equilibrium heat and single adsorbate transfer in fluid flow through a porous medium. II: Predictions for a silica–gel–air-drier using characteristics charts, Chem. Eng. Sci. 27 (1972) 1157–1169.
[23] O.A. Hougen, W.R. Marshall Jr., Adsorption from a fluid stream flowing through a stationary granular bed, Chem. Eng. Prog. 43 (4) (1947) 197–208.
[24] E.R. Gilliland, R.F. Baddour, G. Perkinson, K.J. Sladek, Diffusion on surfaces. I: Effect of concentration on the diffusivity of physically adsorbed gases, Indust. Eng. Chem. Fundament. 13 (2) (1974) 95–100.

[25] M.N. Özişik, Heat Conduction, second ed., Wiley Interscience, New York, 1993.
[26] R.K. Shah, Thermal design theory for regenerators, in: S. Kakaç, A.E. Bergles, F. Mayinger (Eds.), Heat Exchangers: Thermal-Hydraulic Fundamentals and Design, Hemisphere, New York, NY, 1981, pp. 721–763.
[27] R.E. Treybal, Mass-Transfer Operations, McGraw-Hill, 1980.
[28] W.M. Kays, A.L. London, Compact Heat Exchangers, second ed., McGraw-Hill, New York, NY, 1964.
[29] E. Van den Bulck, J.W. Mitchell, S.A. Klein, Design theory for rotary heat and mass exchangers. II: Effectiveness-number-of-transfer-units method for rotary heat and mass exchangers, Int. J. Heat Mass Transfer 28 (8) (1985) 1587–1595.
[30] G.R. Youngquist, Diffusion and flow of gases in porous solids, Indust. Eng. Chem. 62 (8) (1970) 52–63.
[31] D.M. Ruthven, Principles of adsorption and adsorption processes, John Wiley & Sons, New York, NY, 1984.
[32] K.J. Sladek, E.R. Gilliland, R.F. Baddour, Diffusion on surfaces. II: Correlation of diffusivities of physically and chemically adsorbed species, Indust. Eng. Chem. Fundam. 13 (2) (1974) 100–105.
[33] P.L. Brillhart, Evaluation of Desiccant Rotor Matrices Using an Advanced Fixed-Bed Test System, Ph.D. thesis, University of Illinois at Chicago, Chicago, IL, USA, June 1997.
[34] J.L. Niu, L.Z. Zhang, Heat and mass transfer and friction coefficients in corrugated ducts confined by sinusoidal and arc curves, Int. J. Heat Mass Transfer 45 (2002) 571–578.
[35] C.C. Wang, C.T. Chang, Heat and mass transfer for plate fin-and-tube heat exchangers, with and without hydrophilic coating, Int. J. Heat Mass Transfer 41 (1998) 3109–3120.